Published in final edited form as:
Microbes Infect. 2008 June ; 10(7): 726–733. doi:10.1016/j.micinf.2008.03.011.

Helicobacter hepaticus HHGI1 is a pathogenicity island associated with typhlocolitis in B6.129-IL10^{tm1Cgn} mice

Zhongming Ge[a,§], **Torsten Sterzenbach**[b,§], **Mark Whary**[a], **Barry Rickman**[a], **Arlin Rogers**[a], **Zeli Shen**[a], **Nancy S. Taylor**[a], **David B. Schauer**[a], **Christine Josenhans**[b,#], **Sebastian Suerbaum**[b,#], and **James G. Fox**[a,#,*]

a*Division of Comparative Medicine, Massachusetts Institute of Technology, Building 16-825, 77 Massachusetts Ave., Cambridge, MA 02139, USA*

b*Institute of Medical Microbiology and Hospital Epidemiology, Hannover Medical School, Carl-Neuberg-Str. 1, D-30625 Hannover, Germany*

Abstract

Helicobacter hepaticus strain 3B1 (*H. hepaticus*) contains a genomic island of ~71 kb, *HHGI1*, with some of the common features shared among known bacterial pathogenicity islands. In this study, we characterized the pathogenic potential of *HHGI1* by infecting B6.129-IL10^{tm1Cgn} (IL10$^{-/-}$) mice with an isogenic mutant (*namely HhPAId1*) lacking 19 predicted genes within *HHGI1*. In contrast to *H. hepaticus* ($P < 0.001$), *HhPAId1*did not cause typhlocolitis and hyperplasia in IL10$^{-/-}$ mice. Colonization levels of *HhPAId1* were significantly higher in the cecum ($P < 0.007$) and similar in the colon ($P = 0.27$) when compared to *H. hepaticus* by 13 or 16 weeks post inoculation (WPI). The magnitude of the Th1-associated IgG2c response against *HhPAId1* was less than that against *H. hepaticus* ($P < 0.004$). There was no significant difference in Th2-associated IgG1 responses against these two strains. Cecal and colonic mRNA levels of proinflammatory cytokines IFN-γ, TNF-α and IL-17a in the *HhPAId1*-infected mice were significantly lower than those in the *H. hepaticus*-infected mice ($P < 0.05$) at 13 WPI. These results demonstrate that genes in the *HHGI1* contribute to the pathogenicity of *H. hepaticus*, at least in part via up-regulation of proinflammatory mediators IFN-γ, TNF-α and IL-17a.

Keywords

H. HEPATICUS; ISOGENIC MUTANT; PATHOGENICITY ISLAND

1. Introduction

During microbial evolution, many bacterial genomes have acquired blocks of DNA-called "genomic islands" from other organisms by horizontal transfer (reviewed in [1]. These genomic islands can be divided into several subtypes based on their functionality, including ecological islands, saprophytic islands, symbiosis islands and pathogenicity islands (PAI) [1]. PAIs

*Corresponding author: James G. Fox, DVM, Division of Comparative Medicine, Massachusetts Institute of Technology 77 Massachusetts Avenue, 16-825, Cambridge, MA 02139, Tel: 617-253-1735, Fax: 617-258-5708, Email: jgfox@mit.edu
§authors contributed equally
#share senior authorship.

encode one or more virulence-associated factors and often have a G+C content distinct from the rest of the core genome [2]. Bacterial PAIs, such as the well characterized *LEE* in enteropathogenic *Escherichia coli*, *cag* in *Helicobacter pylori* and *SaPI1* in *Staphylococcus aureus*, significantly contribute to the virulence of these pathogens [2].

Helicobacter hepaticus infection leads to chronic hepatitis, hepatocellular carcinoma and typhlocolitis in susceptible mouse strains [3,4]. Recently, it has been demonstrated that this bacterium also contributes to the formation of cholesterol gallstones in C57L/J mice [5], colonic tumors in 129 *Rag2*$^{-/-}$ mice [6], and mammary tumors in *Apc*$^{min+}$ *Rag2*$^{-/-}$ mice [7]. However, our knowledge of virulence factors of this pathogen remains limited; the best characterized *H. hepaticus* virulence factor is cytolethal distending toxin (CDT) which is essential for persistent colonization, and plays an important role in the development of *H. hepaticus*-induced typhlocolitis in C57BL/6 *IL10*$^{-/-}$ mice [8] and hepatic dysplasia in male A/JCr mice [9]. A distinct genomic island of ~71 kb (termed *HHGI1*) comprising 70 predicted genes was identified in the completely sequenced genome of *H. hepaticus* strain 3B1 (ATCC51449) [10]. *HHGI1* displays several features of a bacterial PAI, including its relatively low G+C content as compared to the rest of the chromosome and a prophage P4-like integrase, and also like *H. pylori cagPAI* [11], contains several homologs (*VirB10*, *VirB4*, and *VirD4*) of components of the *Agrobacterium tumefaciens* type IV secretion system (T4SS). In addition, the presence of *HHGI1* genes is highly variable among *H. hepaticus* isolates [10], a phenomenon also observed for the *H. pylori cag* PAI [11]. Importantly, male A/JCr mice infected with *H. hepaticus* strains lacking the entire *HHGI1* (MIT 96-1809 isolated from mice originating in the Netherlands) or ~62 out of 71 kb (MIT 96-284 from mice in Germany) developed less severe hepatitis than those infected with *H. hepaticus* 3B1 containing the intact *HHGI1* [12]. These lines of evidence suggested that *HHGI1* is a candidate PAI for *H. hepaticus*. In this study, we generated an isogenic mutant of *H. hepaticus* 3B1, in which a ~20-kb portion of *HHGI1* containing the *VirB10* and *VirB4* homologs was deleted. The effect of this deletion on colonization, pathogenicity and host proinflammatory responses was investigated in B6.129-IL10^{tm1Cgn} mice.

2. Materials and Methods

2.1. *Helicobacter hepaticus* strains, growth media and conditions

H. hepaticus strain 3B1 (ATCC 51448) [3] was cultured on blood agar (Remel, Lexington, Kn) for 2-3 days under microaerobic conditions (10% H_2, 10% CO_2, 80% N_2). Chloramphenicol (Cm)-resistant *H. hepaticus* mutants were selected on blood agar base supplemented with 10% horse blood and 10 mg/L of Cm.

2.2. Construction of isogenic mutants

In order to construct a mutant of *H. hepaticus* 3B1 where a block of *HHGI1* genes (HH0250-HH0268) was deleted, two regions of approximately 2,000 bp were amplified by PCR, one 5′ of gene HH0250 with the primers hepI1P1fw (5′-cgg**ggtacc**TGTGGCTCATAAGGAGATCG-3′) and hepI1P1rv (ggaagatctATACCATTATACCAAGCGACC) and a second one 3′ of the gene HH0268 with the primers hepI1P2fw (5′-ggaagatctTAACAGGAGTGGTAACACGG-3′) and hepI1P2rv (5′-cgg**ggtacc**AGCAGGTGCATTGCCATTCC-3′). Capital letters in the primer sequences indicate homologous regions to the genome of *H. hepaticus*, bold letters *Kpn*I-sites, and underlined letters *Bgl*II-sites. The PCR products were first digested with *Bgl*II, then one PCR-product was dephosphorylated and both PCR-products were ligated with each other (Fig.1). After cleanup, the ligation product was digested with *Kpn*I and cloned into the *Kpn*I site of pUC18 (pSUS2104). The chloramphenicol acetyltransferase (CAT) cassette of *Campylobacter coli* [13] was PCR-amplified from pBHpC8, digested with *Bam*HI, and subsequently cloned into the compatible *Bgl*II sites created

in pSUS2104, resulting in plasmid pSUS2105. Mutagenesis was performed by transformation of *H. hepaticus* with the mutant construct pSUS2105 by electroporation. Bacteria grown for 24 h on blood agar plates were harvested in electroporation buffer (10% glycerol), and washed two times by centrifugation at 5000 × g for 20 min. Bacteria were than resuspended in electroporation buffer. Bacterial suspension (80 μl) was mixed with 10-25 μg of dialysis-desalted DNA in a volume of 10 μl. . Electroporation was performed with electroporation cuvettes with a gap width of 0.1 cm (Biorad) and the following settings: a capacity of 25 μF, a voltage of 2.5 kV and a resistance of 2000 Ohm, resulting in a time constant between 4 and 4.5 sec. After electroporation, 500 μl of SOC-medium were added and the bacteria were incubated on non-selective blood agar plates for 1 day, followed by transfer of the bacteria to selective blood agar plates containing 10 mg/L Cm, and further incubated until Cm-resistant colonies appeared. These colonies were then propagated on new plates. Genetic characterization on chromosomal DNA isolated from the mutants was performed using PCR and sequencing.

2.3. Experimental design for *in vivo* infection

Male *Helicobacter* spp.-free B6.129-IL10^{tm1Cgn} (IL10$^{-/-}$) mice (4 to 6-week-old) were originally purchased from the Jackson Laboratory (Bar Harbor, ME), rederived by embryo transfer, bred and housed in a specific pathogen-free (including *Helicobacter* spp.) facility. This facility is accredited by the Association for Accreditation and Assessment of Laboratory Animal Care, International. In the first study, the mice housed in static microisolator cages (6 for the control groups and 5 for the infection groups) were infected with *H. hepaticus* 3B1, or its PAI-deficient mutant (*HhPAId1*) in parallel with sham-dosed controls using Brucella broth for 16 weeks. A second study (5 mice per group) with a similar experimental design was performed to test reproducibility of the pathogenic potential of the mutant *HhPAId1*. In this experiment, necropsy was performed at 13 week post inoculation (WPI) due to deteriorating body conditions of the WT *H. hepaticus*-infected mice. For oral gavage, bacteria were cultured on blood agar, resuspended in Brucella broth, and adjusted to 10^9 organisms/ml as estimated by spectrophotometry at OD_{600nm}. Mice received 0.2 ml of fresh inocula by gastric gavage every other day for three doses or sham dosed with Brucella broth.

H. hepaticus infection status was monitored using the Ready-To-Go PCR Bead system (GE Healthcare, Little Chalfont, England) and *H. hepaticus*-specific primers [14]. Immediately after CO_2 euthanasia, blood was obtained and intestinal contents were removed by rinsing with sterile saline. Approximately 1-cm segments of cecum or colon were collected for RNA/DNA isolation. Tissues were frozen in liquid nitrogen immediately after sampling and stored at -70° C prior to use. Representative tissue sections were fixed in 10% buffered formalin for histology.

2.4. ELISA for serum IgG2c and IgG1 responses to *H. hepaticus*

Sera were obtained at necropsy from 10 IL-10$^{-/-}$ mice infected with *HhPAId1* and 9 IL-10$^{-/-}$ mice infected with the WT *H. hepaticus* 3B1. Serum Th1-associated IgG2c and Th2-associated IgG1 responses to outer membrane antigens of *H. hepaticus* 3B1 were measured by ELISA as previously [15]. Antigen was coated on Immulon II plates at a concentration of 10 μg/ml with sera diluted 1:100. Biotinylated secondary antibodies included goat anti-mouse IgG (Southern Biotechnology Associates) and monoclonal anti-mouse antibodies produced by clones A85-1 and 5.7 (PharMingen) for detecting IgG1 and IgG2c, respectively. Incubation with extravidin peroxidase (Sigma) was followed by 2,2′-azinobis (3-ethylbenzthiazoline-6-sulfonic acid) diammonium salt (ABTS®) substrate (Kirkegaard and Perry Laboratories, Gaithersburg, MD) for color development. Absorbance (or optical density) development at 405/562 nm was recorded by an ELISA plate reader (Dynatech MR7000, Dynatech Laboratories, Inc., Chantilly, VA).

2.5. Real-time quantification of *H. hepaticus* and selected cytokines in murine intestinal tissues

Chromosomal DNA from cultured bacteria was prepared using a High Pure PCR Template kit according to the manufacturer's protocol (Roche Applied Science, Indianapolis, IN). Total DNA and RNA from cecum and colon were isolated using Trizol Reagents following the supplier's procedure (Invitrogen). Quantification of *H. hepaticus* in each of the intestinal segments was determined by real-time quantitative PCR (Q-PCR) in the Prism Sequence Detection Systems 7700 (Applied Biosystems) as described elsewhere [16]. The copy numbers of *H. hepaticus* genomes were expressed per μg of mouse DNA whose quantity was determined by using Q-PCR and the 18S rRNA gene-based primers and probe (Applied Biosystems).

For cytokine mRNA quantification, 5 μg of total RNA from samples were converted into cDNA using High Capacity cDNA Archive kit following the supplier's recommendation (Applied Biosystems). The cDNA levels for glyceraldehyde-3-phosphate dehydrogenase (*GAPDH*), *IL-5*, *IL-13*, *IL-17a*, *IL-23a*, *TNFα*, and *IFNγ* mRNA were measured by Q-PCR using commercial primers and probes (Applied Biosystems). Transcript levels were normalized to the endogenous control (*GAPDH*), and expressed as fold change compared with sham-dosed control mice using the Comparative C_T method (Applied Biosystems User Bulletin no. 2).

2.6. Histopathology evaluation

The ileoceco-colic junction and colon were embedded in paraffin, sectioned at 5 μm, and stained with hematoxylin and eosin staining (H&E). Lesions were evaluated by two veterinary pathologists blinded to sample identity. The same scoring system was used as previously described [17].

2.7. Statistical analyses

The two-tailed Student's *t* test or a nonparametric Mann-Whitney *U* test was used for comparing data on the colonization levels of *H. hepaticus*, cytokine mRNA levels and serology, or on histopathological scores. Values of $P < 0.05$ are considered significant.

3. Results

3.1. Construction and characterization of an *H. hepaticus HHGI1* partial deletion mutant

The *HHGI1* island of *H. hepaticus* comprising the open reading frames HH0233-HH0302 presumably presents a pathogenicity island of *H. hepaticus*. This island is partially or completely missing in several clinical isolates of *H. hepaticus* [10] and we documented previously that two of these clinical isolates of *H. hepaticus* missing the *HHGI1* island completely or partially induced a lower degree of hepatitis than a *HHGI1*-containing strain in A/JCr mice [12]. In order to verify that the *HHGI1* island of *H. hepaticus* indeed is a pathogenicity island, a deletion mutant was constructed where the *HHGI1* open reading frames HH0250-HH0268 were deleted. This part of the *HHGI1* island was chosen because it comprises homologs to components of a T4SS, namely VirB10 (HH0252) and VirB4 (HH0260). The mutant was constructed by cloning approximately 2,000 bp of DNA on both sides of the chromosomal region to be deleted into pUC18, interspersed with a gene encoding CAT (Fig. 1). This construct (pSUS2105) was transformed into *H. hepaticus* 3B1 to generate a deletion mutant of HH0250-HH0268 by homologous recombination. The mutant called *HhPAId1* was verified by an empty site PCR using primers binding 3′ and 5′ of the deleted region and by PCR using oligonucleotides binding in the deleted region (not shown). The mutant was examined microscopically and did not show any morphological differences compared to wild type bacteria. Also there were no differences in growth rate (not shown).

3.2. Partial deletion of *HHGI1* did not reduce intestinal colonization levels of *HhPAId1* compared to WT *H. hepaticus*

The successful colonization of WT *H. hepaticus* and *HHGI1*-defective *HhPAId1* in the mice was monitored by fecal PCR at 4 and 8 WPI (data not shown). Colonization levels of *H. hepaticus* 3B1 and *HhPAId1* for two infection experiments were combined and presented in Fig. 2. Deletion of the genetic locus containing HH0250 - HH0268 within the *H. hepaticus HHGI1* did not decrease colonization levels of the mutant in the cecum and colon when compared to *H. hepaticus* 3B1. In fact, the colonization level of the mutant in the ceca was significantly higher ($P = 0.007$) than of *H. hepaticus* 3B1, whereas their levels were not significantly different in the colon.

3.3. *HHGI*-defective mutant lacks the ability to induce intestinal pathology

Mice infected with *H. hepaticus* 3B1 developed significantly more severe inflammation and hyperplasia in the cecocolic junction and the distal colon compared to mice infected with *HhPAId1* (Fig. 3.1, $P < 0.001$). Seven of nine uninfected mice and 10 of 10 *HhPAId1*-infected mice had normal-appearing ceca and colons (not shown), with no development of typhlocolitis, hyperplasia or crypt atrophy after 13-16 WPI (Fig. 3.1 and 3.2). One mouse from the sham control group of each experiment also developed intestinal pathology comparable to the WT *H. hepaticus*-infected mice in the large bowel (Fig. 3.1); the development of these clinical presentations appeared to be spontaneous since *H. hepaticus* was not detected in the sham control mice by Q-PCR (data not shown). In contrast, in the WT *H. hepaticus*-infected group all 10 mice developed a moderate typhlitis, along with hyperplasia, crypt necrosis, mild crypt atrophy, early mild dysplastic glandular epithelium, submucosal inflammation and follicle formation and accompanying edema and ectatic lymphatic vessels (Fig. 3.2, C, D). Although lesions were most severe in the cecal-colic junction, the middle and distal colon had mild inflammation, occasional submucosal edema, and mild hyperplasia of the epithelium (not shown).

3.4. Th1 or Th2-associated serum IgG isotype responses to *H. hepaticus*

The serological data combined from the two in vivo experiments demonstrated that the IL-$10^{-/-}$ mice infected with *HhPAId1* or *H. hepaticus* 3B1 developed significantly higher levels of both Th1-associated IgG2c and Th2-associated IgG1 responses to *H. hepaticus* compared to the sham controls (Fig. 4, $P < 0.0001$). In addition, the *H. hepaticus* - specific Th1-associated IgG2c response of the mice infected with *H. hepaticus* 3B1 was significantly higher than the mice infected with *HhPAId1* ($P < 0.004$), whereas there was no significant difference in the Th2-associated IgG1 responses to either infection (Fig. 4, $P=0.14$).

3.5. Partial deletion of *HHGI1* diminished WT *H. hepaticus*-promoted host proinflammatory responses

Previous studies demonstrated that WT *H. hepaticus* infection is associated with Th1 cell-mediated immune responses and stimulates the production of TNF-α and IFN-γ [15,18]. To dissect how the partial deletion of *HHGI1* affects host immune responses, we measured cecal and colonic mRNA levels of 4 Th1/Th17 cytokines, including IL-17a, IL-23a, TNF-α and IFN-γ, as well as two Th2 cytokines, IL-5 and IL-13, in the second experiment (Fig. 5). *H. hepaticus* 3B1 infection significantly up-regulated mRNA levels of IL-17a ($P = 0.028$ for the cecum and <0.05 for the colon), TNF-α ($P = 0.0003$ for the cecum and $P < 0.05$ for the colon) and IFN-γ ($P = 0.0008$ for the cecum and $P=0.012$ for the colon) when compared to the *HHGI1*-defective *HhPAId1* infection; in contrast, there was no significant difference in the mRNA levels of IL-23a between the WT *H. hepaticus*- and the *HhPAId1*-infected groups (Fig. 5). The mRNA levels of cecal IL-17a were significantly higher in the both infected groups than the controls (Fig. 5). In spite of the notable higher levels on mean folds of the *TNF-α* and *IFN-*

γ mRNA in the *H. hepaticus* 3B1-infected mice compared to the sham-dosed mice, they were statistically insignificant, which is due to the spontaneous inflammation that developed in one of four control mice, leading to the large standard deviation of the data for the control mice (Fig. 5). After removal of this mouse from the control group, the mRNA levels of cecal or colonic *TNF-α* and *IFN-γ* between the control mice and the mice infected with WT *H. hepaticus* but not with *HhPAId1* were significantly different ($P < 0.05$, data not shown). For Th2 cytokines, *H. hepaticus* 3B1 infection induced significantly higher cecal mRNA levels of IL-5 and IL-13 than *HhPAId1* infection or the sham control (Fig. 5, $P < 0.05$); the mRNA levels of these two cytokines in the colon were not significantly different between the groups.

4. Discussion

The ~71 kb genomic island *HHGI1* present in the genome of *H. hepaticus* ATCC51449 displays many common features of bacterial PAIs and was proposed as a candidate PAI for *H. hepaticus* [10]. Our previous study demonstrating that *H. hepaticus* strains naturally lacking the entire or partial *HHGI1* induced less severe chronic hepatitis in A/JCr mice provides supporting evidence for this proposal [12]. Here we demonstrate that the partial deletion of *HHGI1* abolished the ability of *H. hepaticus* to induce typhlocolitis and hyperplasia in $IL10^{-/-}$ mice in contrast to *H. hepaticus* 3B*1*, linking *HHGI1* to the pathogenicity of *H. hepaticus*. These collective data strongly indicate that *HHGI1* is a pathogenicity island for *H. hepaticus*.

The region deleted from *HHGI1* was not required for *H. hepaticus* colonization in the large bowel. This result is similar to the previous finding that the *H. pylori cag*PAI is dispensable for colonization in mice and piglets [19]. Interestingly, the mean colonization level of the *HHGI1*-deficient *HhBac26* was significantly higher than that for *H. hepaticus* 3B1. The lower colonization density reached by *H. hepaticus* 3B1 compared to *HhPAId1* in the cecum may result from up-regulation of proinflammatory mediators such as IFN-γ by *H. hepaticus* 3B1. A similar up-regulation of proinflammatory mediators has been demonstrated to promote clearance of *H. pylori* and *Yersinia enterocolitica* from mice [20-22]. These data are supported by our previous finding that ceca of hepatitis-resistant C57BL/6 mice contains more *H. hepaticus* organisms (~100-fold) than chronic hepatitis/typhlocolitis-prone A/JCr mice [15, 23,24].

Although the colonization levels of *HhPAId1* in the cecum were higher than those of *H. hepaticus* 3B1, the *H. hepaticus*-specific Th1-associated IgG2c responses to the mutant were significantly lower than to WT *H. hepaticus* infection, suggesting that the gene products encoded by *HHGI1* are important for causing proinflammatory Th1-type host responses to infection. Importantly, this isogenic mutant lost its ability to induce intestinal pathology and also did not up-regulate mRNA levels of IFN-γ and TNF-α when compared to WT *H. hepaticus*. IFN-γ and TNF-α are pleiotropic proinflammatory mediators involving multiple cellular functions. For example, TNF-α modulates a proinflammatory NF-κB pathway and apoptosis, and IFN-γ enhances natural killer cell and macrophage activity against microbial infection as well as regulation of B cell functions (reviewed in Ref. [25,26]. It has been thoroughly documented that up-regulation of IFN-γ and TNF-α are often associated with *H. hepaticus*-induced diseases in susceptible murine models [7,15,18,23,27,28]. In addition, neutralization of IFN-γ inhibited the development of *H. hepaticus*-induced typhlocolitis in C57BL/10 $IL10^{-/-}$ and C57BL/10 $Rag^{-/-}$ mice [18,27]; treatment with anti-TNF-α antibody suppresses intestinal tumors induced by *H. hepaticus* infection in C57BL/6J $Rag2^{-/-}Apc^{Min/+}$ mice [7]. These findings indicate the importance of IFN-γ and TNF-α in the pathogenesis of *H. hepaticus*-induced diseases. It is worth noting that the mRNA levels of *IL-5* and *IL-13* were significantly higher in the WT *H. hepaticus*-infected ceca affected by severe inflammation compared to the *HHGI1*-deficient mutant-infected or sham dosed mice. These findings are

likely due to compensatory host responses to counteract the induced tissue injuries and is consistent with a previous study reporting up-regulation of both Th1- and Th2-type cytokines in *H. hepaticus*-infected A/JCr mice [23]. Therefore, the results from this study ascertain that *HHGI1* contributes to pathogenicity of *H. hepaticus*, at least in part, by up-regulating expression of IFN-γ and TNF-α and a Th1 response.

Recently, cytokines IL-23 and IL-17 have been demonstrated to play a pivotal role in innate immunity and T cell - mediated intestinal inflammation in immune-deficient mouse models [29] [28]. Neutralization of IL-23 or knockout of the *IL-23* gene diminishes intestinal inflammation as well as elevated production of IL-17 induced by *H. hepaticus* infection or by adoptive transfer of effector CD4+ T cells in C57BL/6 *Rag*$^{-/-}$ mice [28]. Current evidence indicates that IL-23 is critical for IL-17-expressing Th17 function in vivo [30]. In this study, mRNA expression of cecal and colonic IL-17a was significantly increased by WT *H. hepaticus* infection compared to *HhPAId1* infection (Fig. 5); however, no significant differences in mRNA levels of IL-23a were noted among the *H. hepaticus* 3B1-infected, the *HhPAId1*-infected and the sham control groups (Fig. 5). Intriguingly, the mRNA level of cecal IL-17 in the *HhPAId1*-infected mice was higher by 25-fold than that in the sham controls (Fig. 5), suggesting that additional factors from the remaining portion of *HhPAId1* or other virulence properties are also involved the transcriptional up-regulation of *IL-17a*. We hypothesize that the *H. hepaticus*-associated up-regulation of the *IL-17a* mRNA is induced by an alternative pathway proposed by Weaver *et al* [30], in which IL-17 production could be induced directly by T cell receptor stimulation by bacterial antigens independent of IL-23. Further investigations are required for testing this hypothesis.

In summary, our data provided strong evidence supporting that *HHGI1* is a *H. hepaticus* pathogenicity island [10]. Infection with this *HhPAI* mutant in other rodent models such as A/JCr mice for liver tumor development and *Rag2*$^{-/-}$ mice for progression of colitis to lower bowel cancer will further delineate virulence properties of *HHGI1*. This conclusion also opens an avenue for further characterizing virulence factors encoded by *HHGI1* and comparing the pathogenic strategies utilized by different helicobacters (e.g, *H. hepaticus* versus *H. pylori*) to trigger inflammation and tumorigenesis in these respective hosts.

5. Acknowledgements

This project was financially supported by NIH grants R01 CA67529, P30ES02109 (J.G.F.) R01 DK52413 (DBS), and by grant SFB621/B8 from the Deutsche Forschungsgemeinschaft (S.S.) and by the PathoGenoMik initiative of the German Ministry for Education and Research (S.S. and C.J.).

References

[1]. Hacker J, Carniel E. Ecological fitness, genomic islands and bacterial pathogenicity. A Darwinian view of the evolution of microbes. EMBO Rep 2001;2:376–381. [PubMed: 11375927]

[2]. Gal-Mor O, Finlay BB. Pathogenicity islands: a molecular toolbox for bacterial virulence. Cell. Microbiol 2006;8:1707–1719. [PubMed: 16939533]

[3]. Fox JG, Dewhirst FE, Tully JG, Paster BJ, Yan L, Taylor NS, Collins MJ Jr. Gorelick PL, Ward JM. *Helicobacter hepaticus* sp. nov., a microaerophilic bacterium isolated from livers and intestinal mucosal scrapings from mice. J. Clin. Microbiol 1994;32:1238–1245. [PubMed: 8051250]

[4]. Rogers AB, Fox JG. Inflammation and Cancer. I. Rodent models of infectious gastrointestinal and liver cancer. Am. J. Physiol 2004;286:G361–366.

[5]. Maurer KJ, Ihrig MM, Rogers AB, Ng V, Bouchard G, Leonard MR, Carey MC, Fox JG. Identification of cholelithogenic enterohepatic helicobacter species and their role in murine cholesterol gallstone formation. Gastroenterology 2005;128:1023–1033. [PubMed: 15825083]

[6]. Erdman SE, Poutahidis T, Tomczak M, Rogers AB, Cormier K, Plank B, Horwitz BH, Fox JG. CD4$^+$ CD25$^+$ regulatory T lymphocytes inhibit microbially induced colon cancer in *Rag2*-deficient mice. Am. J. Pathol 2003;162:691–702. [PubMed: 12547727]

[7]. Rao VP, Poutahidis T, Ge Z, Nambiar PR, Boussahmain C, Wang YY, Horwitz BH, Fox JG, Erdman SE. Innate immune inflammatory response against enteric bacteria *Helicobacter hepaticus* induces mammary adenocarcinoma in mice. Cancer Res 2006;66:7395–7400. [PubMed: 16885333]

[8]. Young VB, Knox KA, Pratt JS, Cortez JS, Mansfield LS, Rogers AB, Fox JG, Schauer DB. In vitro and in vivo characterization of *Helicobacter hepaticus* cytolethal distending toxin mutants. Infect. Immun 2004;72:2521–2527. [PubMed: 15102759]

[9]. Ge Z, Rogers AB, Feng Y, Lee A, Xu S, Taylor NS, Fox JG. Bacterial cytolethal distending toxin promotes the development of dysplasia in a model of microbially induced hepatocarcinogenesis. Cell. Microbiol 2007;9:2070–2080. [PubMed: 17441986]

[10]. Suerbaum S, Josenhans C, Sterzenbach T, Drescher B, Brandt P, Bell M, Droge M, Fartmann B, Fischer HP, Ge Z, Horster A, Holland R, Klein K, Konig J, Macko L, Mendz GL, Nyakatura G, Schauer DB, Shen Z, Weber J, Frosch M, Fox JG. The complete genome sequence of the carcinogenic bacterium *Helicobacter hepaticus*. P. Natl. Acad. Sci. U.S.A 2003;100:7901–7906.

[11]. Censini S, Lange C, Xiang Z, Crabtree JE, Ghiara P, Borodovsky M, Rappuoli R, Covacci A. *cag*, a pathogenicity island of *Helicobacter pylori*, encodes type I-specific and disease-associated virulence factors. P. Natl. Acad. Sci. U.S.A 1996;93:14648–14653.

[12]. Boutin SR, Shen Z, Rogers AB, Feng Y, Ge Z, Xu S, Sterzenbach T, Josenhans C, Schauer DB, Suerbaum S, Fox JG. Different *Helicobacter hepaticus* strains with variable genomic content induce various degrees of hepatitis. Infect. Immun 2005;73:8449–8452. [PubMed: 16299349]

[13]. Wang Y, Taylor DE. Chloramphenicol resistance in *Campylobacter coli*: nucleotide sequence, expression, and cloning vector construction. Gene 1990;94:23–28. [PubMed: 2227449]

[14]. Shames B, Fox JG, Dewhirst F, Yan L, Shen Z, Taylor NS. Identification of widespread *Helicobacter hepaticus* infection in feces in commercial mouse colonies by culture and PCR assay. J. Clin. Microbiol 1995;33:2968–2972. [PubMed: 8576355]

[15]. Whary MT, Morgan TJ, Dangler CA, Gaudes KJ, Taylor NS, Fox JG. Chronic active hepatitis induced by *Helicobacter hepaticus* in the A/JCr mouse is associated with a Th1 cell-mediated immune response. Infect. Immun 1998;66:3142–3148. [PubMed: 9632578]

[16]. Ge Z, Feng Y, Whary MT, Nambiar PR, Xu S, Ng V, Taylor NS, Fox JG. Cytolethal distending toxin is essential for *Helicobacter hepaticus* colonization in outbred Swiss Webster mice. Infect. Immun 2005;73:3559–3567. [PubMed: 15908385]

[17]. Erdman SE, Sohn JJ, Rao VP, Nambiar PR, Ge Z, Fox JG, Schauer DB. CD4$^+$ CD25$^+$ regulatory lymphocytes induce regression of intestinal tumors in Apc$^{Min/+}$ mice. Cancer Res 2005;65:3998–4004. [PubMed: 15899788]

[18]. Kullberg MC, Ward JM, Gorelick PL, Caspar P, Hieny S, Cheever A, Jankovic D, Sher A. *Helicobacter hepaticus* triggers colitis in specific-pathogen-free interleukin-10 (IL-10)-deficient mice through an IL-12- and gamma interferon-dependent mechanism. Infect. Immun 1998;66:5157–5166. [PubMed: 9784517]

[19]. Eaton KA, Kersulyte D, Mefford M, Danon SJ, Krakowka S, Berg DE. Role of *Helicobacter pylori* cag region genes in colonization and gastritis in two animal models. Infect. Immun 2001;69:2902–2908. [PubMed: 11292705]

[20]. Autenrieth IB, Beer M, Bohn E, Kaufmann SH, Heesemann J. Immune responses to *Yersinia enterocolitica* in susceptible BALB/c and resistant C57BL/6 mice: an essential role for gamma interferon. Infect. Immun 1994;62:2590–2599. [PubMed: 8188382]

[21]. Autenrieth IB, Kempf V, Sprinz T, Preger S, Schnell A. Defense mechanisms in Peyer's patches and mesenteric lymph nodes against *Yersinia enterocolitica* involve integrins and cytokines. Infect. Immun 1996;64:1357–1368. [PubMed: 8606101]

[22]. Lee CW, Rao VP, Rogers AB, Ge Z, Erdman SE, Whary MT, Fox JG. Wild-type and Interleukin-10-deficient regulatory T cells reduce effector T-cell-mediated gastroduodenitis in *Rag2*$^{-/-}$ Mice, but only wild-type regulatory T cells suppress *Helicobacter pylori* gastritis. Infect. Immun 2007;75:2699–2707. [PubMed: 17353283]

[23]. Livingston RS, Myles MH, Livingston BA, Criley JM, Franklin CL. Sex influence on chronic intestinal inflammation in *Helicobacter hepaticus*-infected A/JCr mice. Comparative Med 2004;54:301–308.

[24]. Myles MH, Livingston RS, Livingston BA, Criley JM, Franklin CL. Analysis of gene expression in ceca of *Helicobacter hepaticus*-infected A/JCr mice before and after development of typhlitis. Infect. Immun 2003;71:3885–3893. [PubMed: 12819073]

[25]. Schroder K, Hertzog PJ, Ravasi T, Hume DA. Interferon-gamma: an overview of signals, mechanisms and functions. J. Leukocyte Biol 2004;75:163–189. [PubMed: 14525967]

[26]. Papa S, Zazzeroni F, Bubici C, Jayawardena S, Alvarez K, Matsuda S, Nguyen DU, Pham CG, Nelsbach AH, Melis T, De Smaele E, Tang WJ, D'Adamio L, Franzoso G. Gadd45β mediates the NF-κB suppression of JNK signalling by targeting MKK7/JNKK2. Nat. Cell Biol 2004;6:146–153. [PubMed: 14743220]

[27]. Kullberg MC, Jankovic D, Feng CG, Hue S, Gorelick PL, McKenzie BS, Cua DJ, Powrie F, Cheever AW, Maloy KJ, Sher A. IL-23 plays a key role in *Helicobacter hepaticus*-induced T cell-dependent colitis. J. Exp. Med 2006;203:2485–2494. [PubMed: 17030948]

[28]. Hue S, Ahern P, Buonocore S, Kullberg MC, Cua DJ, McKenzie BS, Powrie F, Maloy KJ. Interleukin-23 drives innate and T cell-mediated intestinal inflammation. J. Exp. Med 2006;203:2473–2483. [PubMed: 17030949]

[29]. Yen D, Cheung J, Scheerens H, Poulet F, McClanahan T, McKenzie B, Kleinschek MA, Owyang A, Mattson J, Blumenschein W, Murphy E, Sathe M, Cua DJ, Kastelein RA, Rennick D. IL-23 is essential for T cell-mediated colitis and promotes inflammation via IL-17 and IL-6. J. Clin. Invest 2006;116:1310–1316. [PubMed: 16670770]

[30]. Weaver CT, Hatton RD, Mangan PR, Harrington LE. IL-17 family cytokines and the expanding diversity of effector T cell lineages. Annu. Rev. Immunol 2007;25:821–852. [PubMed: 17201677]

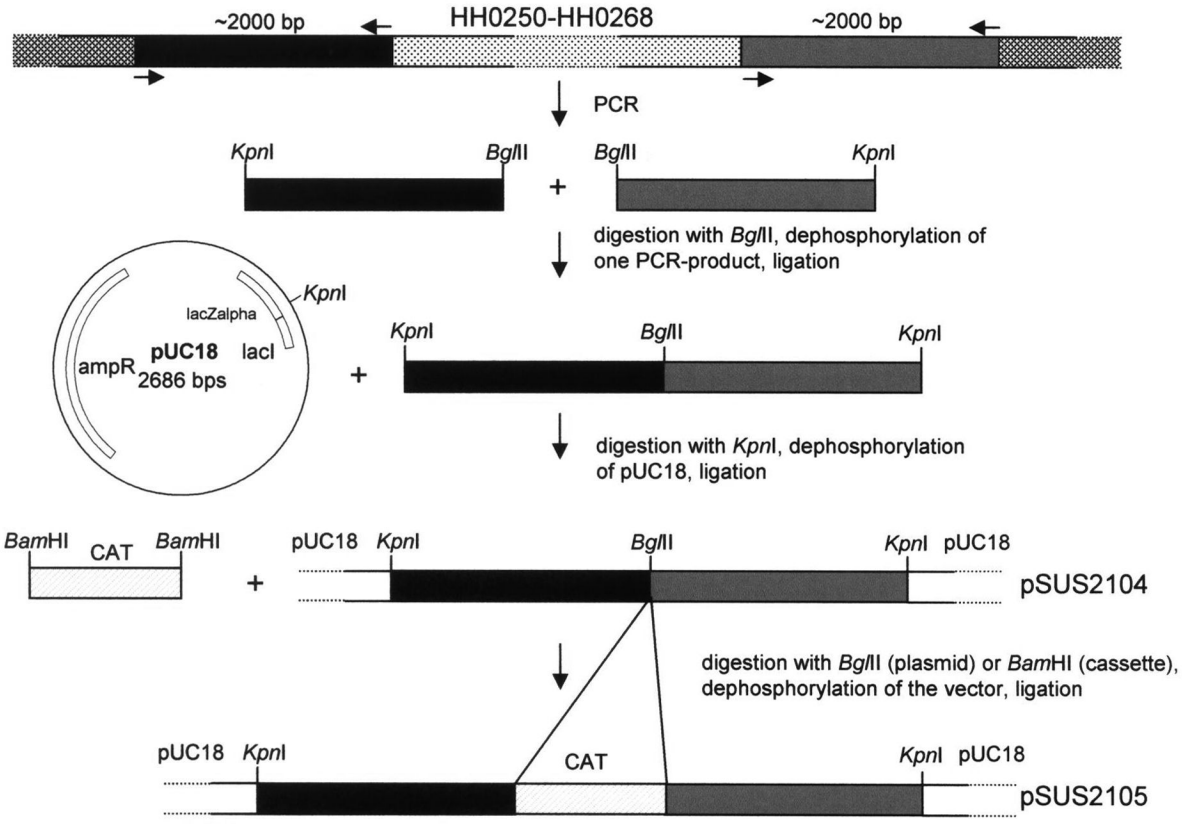

Figure 1.

Construction of an isogenic deletion mutant within *HHGI1*. The hatched region denotes the genetic locus (HH0250 to HH0268, ~21.7 kb) that was replaced with the *Campylobacter coli* chloramphemicol acetyltransferase gene (*CAT*) [13]. HH0252 and HH0246 in the deleted island segment display sequence similarity to *Agrobacterium tumefaciens VirB10* and *VirB4*, respectively [10].

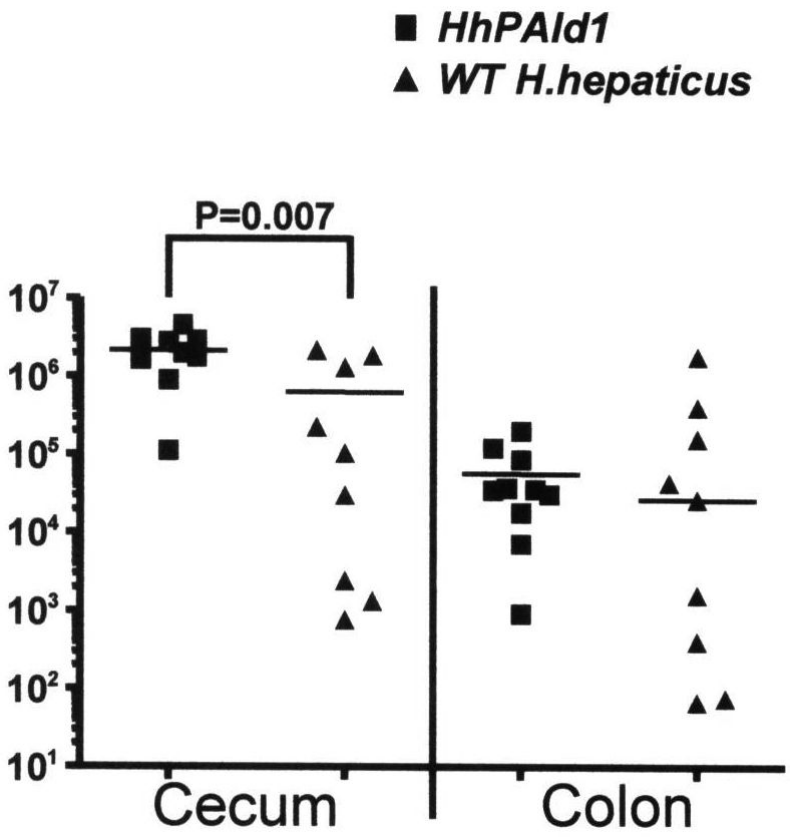

Figure 2.
Colonization levels of *HhPAId1* and WT *H. hepaticus* in the large bowel determined using Q-PCR. Numbers on the y axis represent the genome copies of *H. hepaticus* per μg mouse DNA.

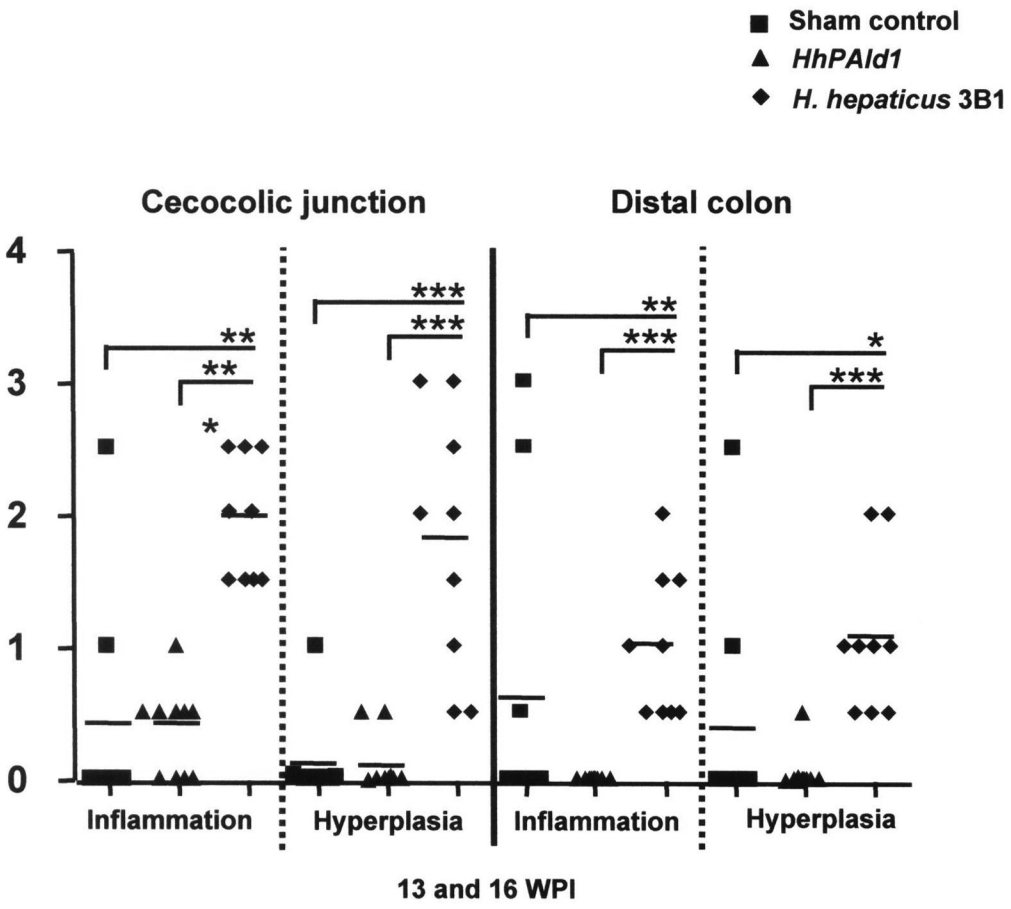

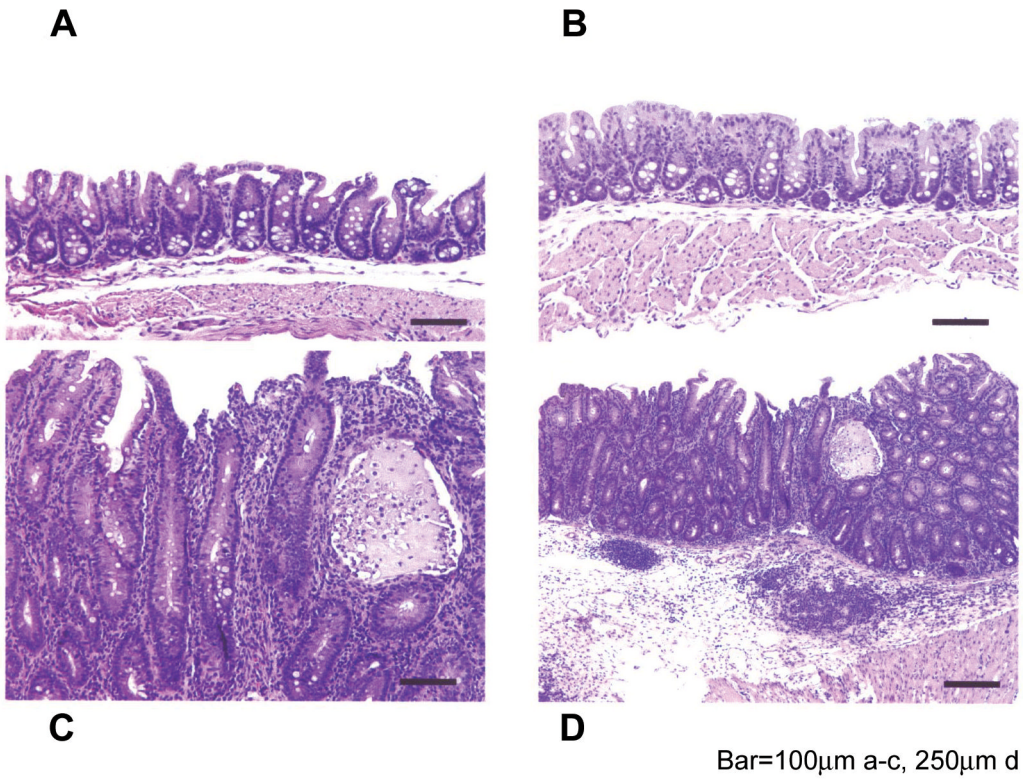

Figure 3.

Histopathological comparison among the mice infected with *HhPAId1*, WT *H. hepaticus* or sham dosed. **3.1**. Pathological scores for the individual mice from the respective groups. P values, *< 0.05, **<0.01, *** <0.001. **3.2**. H&E staining demonstrating representative pathological feaures. A nomal cecum from helicobacter-free male mouse. B. Normal cecum from a *HhPAId1*-infected mouse. C. Moderate diffuse typhlitis with glandular hyperplasia, mild glandular dysplasia, crypt atrophy, loss of goblet cells, a crypt abcess, and attenuated epithelium from *H. hepaticus* 3B1-infected mouse. D. Lower magnification of lesion in C; showing moderate mucosal inflammation and hyperplasia with submucosal inflammation and follicular formation along with severe submucosal edema and dilated lymphatic vessels. Bar = 100 μm in A-C, 250 μm in D.

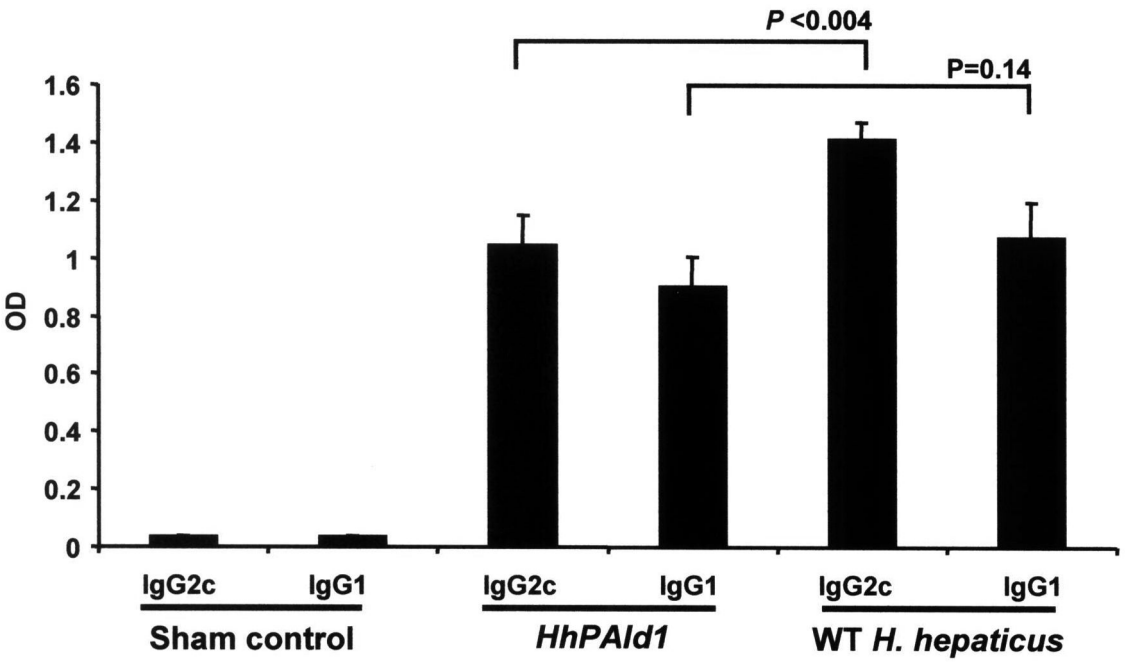

Figure 4.

Sera obtained at necropsy from 10 *IL-10*$^{-/-}$ mice infected with *HhPAId1*, and 9 *IL-10*$^{-/-}$ mice infected WT *H. hepaticus*. The Th1-associated IgG2c response to *H. hepaticus* antigens was lower in mice colonized by the mutant *HhPAId1* ($p<0.004$). The Th2-associated IgG1 responses were equivalent ($p=0.14$). C represents uninfected control mice (n=10). Data represent mean ± standard error.

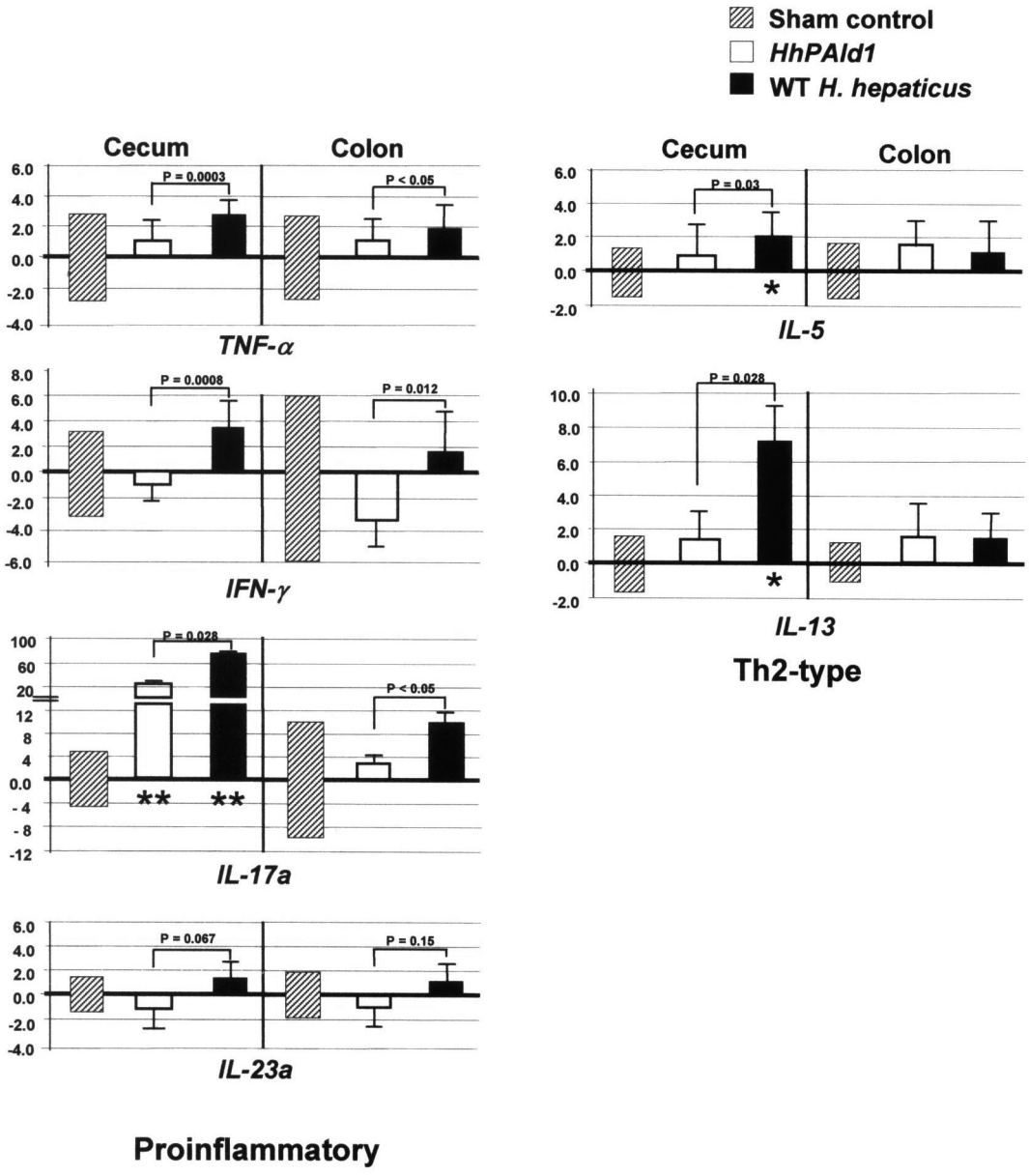

Figure 5.

Relative mRNA levels of proinflammatory and inflammation-suppressive mediators determined by relative Q-PCR. The target mRMA was normalized to that of the "house-keeping: gene" *Gapdh*. Numbers represent mean fold change of the individual mRNA levels in reference to the control group (defined as 0 meaning no change) whose standard deviations of the individual cytokines are represented with the hatched boxes. Bars, standard deviations for the infection groups. P values when compared to the controls: * <0.05, **<0.01.